COMPENSATING FREQUENCY DRIFT IN DPSK SYSTEMS VIA BASEBAND SIGNAL PROCESSING

Zae Yong Choi and Yong Hoon Lee
Dept. of Electrical Engineering
Korea Advanced Institute of Science and Technology
373-1 Kusong-dong, Yusong-gu, Taejon, 305-701, Korea

Abstract

A new baseband signal processing method for compensating frequency shift in DPSK systems is introduced. This method consists of a signal processor for initial aquisition of frequency shift and a simple adaptive equalizer for tracking. The former is based on the observation that the effect of frequency shift can be eliminated by using boundary values of the received baseband signal between symbol periods. The latter is a single tap equalizer employing least mean square (LMS) adaptation algorithm. Computer simulation results demonstrate that the proposed frequency shift compensation technique outperforms existing methods and works well for a wide range of frequency shifts.

I. Introduction

In DPSK the performance of non-coherent detection severely degrades if the carrier frequency at the receiver deviates from its original value due to either the limited oscillator precision or the Doppler effect [1]-[3]. One common way of dealing with this limitation is to employ a conventional automatic frequency control (AFC) loop [4]. Use of such an AFC loop, however , is not recommended in some applications where data are transmitted in bursts, as in time division multiple access (TDMA) systems, because the time to acquire AFC may take a significant portion of the burst interval. For such applications, some alternative methods have been developed: a technique which estimates the phase shift by observing the phase change over half a symbol within each symbol interval was proposed in [5], and one-tap adaptive equalizers correcting the frequency drift at baseband were proposed in [6]-[8]. These techniques have been shown to be useful for compensating some frequency shift; however, their performance rapidly degrades as frequency shift increases.

In this paper, we introduce a new baseband signal processing method that can correct much heavier frequency shift by incorporating the adaptive equalizer in [6] together with a novel acquisition scheme. The latter is based upon realizing that the effect of frequency shift can be eliminated by using *boundary* values of the received baseband signal between symbol periods when rectangular pulses are transmitted. Thus, after converting each received pulse into a rectangular shaped one, we estimate such boundary values from Nyquist rate (twice of symbol rate) samples of received baseband signals, and use them for initial acquisition of frequency shift. It will be shown through simulation that the proposed frequency shift compensation technique outperforms existing methods and performs well for a wide range of frequency shifts.

II. Frequency Shift Compensation Using An Equalizer [6]

Suppose that the input to the receiver shown in Fig.1 is a frequency-shifted DPSK signal expressed as

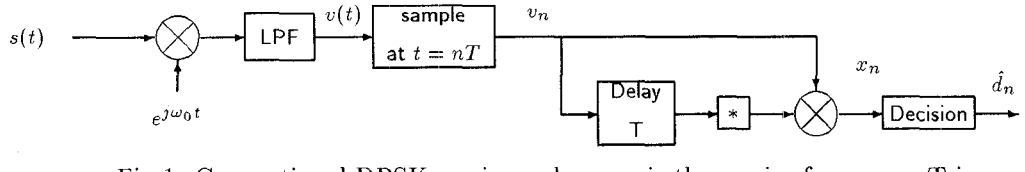

Fig.1. Conventional DPSK receiver where ω_0 is the carrier frequency, T is the symbol period, and '*' denotes the complex conjugate.

0-7803-3682-8/96 $5.00 © 1996 IEEE

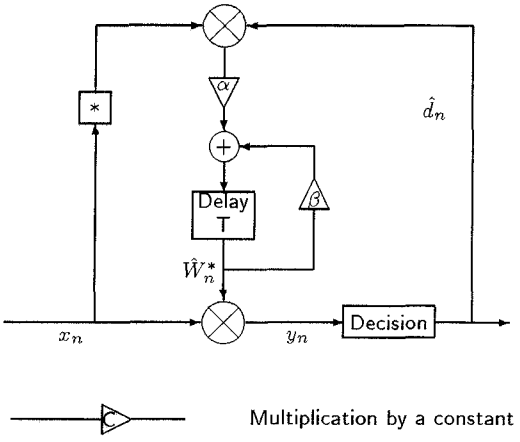

Fig.2. The feedback-frequency drift compensator. Here $x_n = d_n \cdot e^{i\Delta\omega T}$ in (1) , $\beta = 1 - \alpha$ and '*' denotes the complex conjugate.

$$s(t) = \sqrt{2E_s/T}\sin\{(\omega_0 + \Delta\omega)t + \theta(t) + \theta_0\} \quad (1)$$

where E_s and T denote symbol energy and duration, respectively, $\Delta\omega = 2\pi\Delta f$ is the frequency shift in radian, $\Delta\omega \ll \frac{2\pi}{T}$, $\theta(t)$ is M-ary DPSK modulation with symbol rate $1/T$, and θ_0 is the initial phase. Here, for the time being, we assume that the channel is ideal – the received signal $s(t)$ is noise-free and there is no multipath fading. The input x_n to the decision device in Fig. 1 is expressed as

$$x_n = d_n \cdot e^{j\Delta\omega T} \quad (2)$$

where $d_n = e^{j(\theta_n - \theta_{n-1})}$ and $\theta_n = \theta(nT)$. For the binary case $\theta_n - \theta_{n-1}$ is either 0 or π, and the worst case occurs when $\Delta\omega T = \pi$. The one-tap adaptive equalizer in [6], called the feedback-frequency drift compensator (FB-FDC), correcting the effect of $\Delta\omega$ is shown in Fig. 2. The input to the decision device denoted by y_n in Fig.2 is given by

$$y_n = x_n \cdot \hat{W}_n^* \quad (3)$$

where

$$\hat{W}_n^* = (1-\alpha)\hat{W}_{n-1}^* + \alpha x_{n-1}^* \hat{d}_{n-1}; \quad (4)$$

$0 < \alpha < 1$, $\hat{W}_n$ and $\hat{d}_n$ are the estimates of $e^{j\Delta\omega T}$ and d_n, respectively, at time n and $*$ denotes the complex conjugate. This equalizer was designed to minimize the mean squared error between d_n and y_n. Note that $y_n = d_n$ when $\hat{W}_n = e^{j\Delta\omega T}$, since $|e^{j\Delta\omega T}| = 1$. The tap adaptation in (4) is in fact a *least mean square* (LMS) algorithm [9]. Due to the lack of a training sequence, this equalizer works well only when $\Delta\omega$ is small.

III. Detection Through Boundary-Value Estimation

A. Rectangular Pulse Case

Suppose that at the transmitter rectangular baseband pulses are directly multiplied with a carrier without pulse shaping. Then $\theta(t)$ in (1) is constant over a symbol period and $v(t)$ in Fig.1 is given by

$$v(t) = e^{j\theta(t)} \cdot e^{j\Delta\omega t} \cdot e^{j\theta_0}. \quad (5)$$

The phase of x_n in Fig.1 is

$$arg(v_n) - arg(v_{n-1}) = \theta_n - \theta_{n-1} + \Delta\omega T \quad (6)$$

where $arg(v_n)$ denotes the phase of $v_n = v(nT)$. Next we show that the performance degradation caused by $\Delta\omega T$ can be eliminated by considering boundary values of $v(t)$ between symbol periods. The boundary values can be defined as $b_n^i = \lim_{\epsilon\to 0} v(nT - T/2 + \epsilon)$, and $b_n^f = \lim_{\epsilon\to 0} v(nT + T/2 - \epsilon)$, for $\epsilon > 0$ where i and f, respectively, mean initial and final values at the n-th symbol period. The phase difference between b_n^i and b_{n-1}^f is expressed as

$$arg(b_n^i) - arg(b_{n-1}^f) = \theta_n - \theta_{n-1} \quad (7)$$

Thus the effect of frequency shift is indeed removed. As an example, consider the phase of $v(t)$ shown in Fig.3 where $\theta_n - \theta_{n-1} = -\pi$, $\Delta\omega T = 0.5\pi$, $\theta_{n-1} = 0.5\pi$ and $\theta_0 = 0$. From this figure, we can see that $arg(v_n) - arg(v_{n-1}) = -\pi/2$ whereas $arg(b_n^i) - arg(b_{n-1}^f) = -\pi$.

Demodulation of DPSK signals using b_n^i and b_{n-1}^f would be a useful alternative to the conventional scheme in Fig.1. These boundary values, however, cannot be obtained through direct sampling of $v(t)$ at $nT - T/2$. They should be estimated from their neighboring values, which requires a sampling rate higher than the symbol rate 1/T. We consider the sampling of $v(t)$

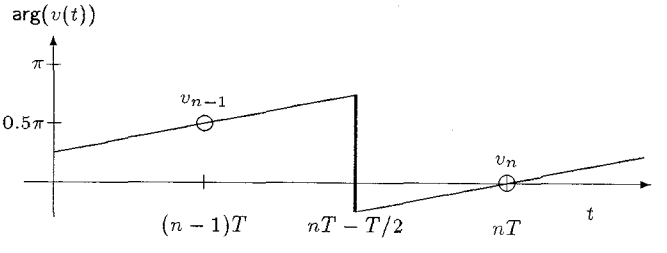

Fig.3. The phase of $v(t)$ when $\theta_n - \theta_{n-1} = -\pi$, $\Delta\omega T = 0.5\pi$, $\theta_{n-1} = 0.5\pi$ and $\theta_0 = 0$.

at the Nyquist rate 2/T. Let v_n^1 and v_n^2, respectively, denote the samples of $v(t)$ at $t = nT - T/2 + t_0$ and $t = nT + t_0$ for $0 < t_0 < T/2$. Estimates of b_n^i and b_n^f can be obtained by *least squares* estimation based on the *linear regression* model [10] using v_n^1 and v_n^2 values. Minimizing the least squares error $\sum_{k=1}^{2}[v_n^k - A(nT - T + kT/2 + t_0) + B]^2$ results in

$$A = (v_n^2 - v_n^1)/\frac{T}{2}; B = v_n^1 - (nT - \frac{T}{2} + t_0)A. \quad (8)$$

This line $At + B$ is merely the line connecting v_n^1 and v_n^2. We can estimate b_n^i and b_n^f by putting $t = nT - T/2$ and $t = nT + T/2$ into $At + B$. The results are

$$\hat{b}_n^i = v_n^1 - At_0; \quad \hat{b}_n^f = 2v_n^2 - v_n^1 - At_0. \quad (9)$$

The DPSK demodulation technique using $\hat{b}_n^i$ and $\hat{b}_n^f$ values will be referred to as the *boundary−based* detection.

B. Raised Cosine Pulse Case

In practical communication systems, rectangular pulses are often converted into raised cosine pulses having bandlimited spectrum before transmission. For such systems, we convert received raised cosine pulses into rectangular ones before applying the boundary-based detection scheme.

For raised cosine pulses, it is desirable to sample at nT, because in the n-th symbol period nT is the only position whose signal value is not corrupted by ISI (Inter Symbol Interference) resulting from pulse shaping. Therefore we sample $v(t)$ at $t = nT$ and $t = nT - T/2$. In this case, unlike the rectangular pulse case, we can sample at $t = nT - T/2$ because sharp transition between symbol periods does not exist. Note that t_0 in (8) and (9) becomes zero. The sampled values, denoted by $v_n^1 = v(nT - T/2)$ and $v_n^2 = v(nT)$ are expressed as

$$v_n^1 = \sum_{k=-\infty}^{\infty} p\{(k - 0.5)T\}e^{j\theta_{n-k}}e^{j(\Delta\omega(n-0.5)T+\theta_0)}; \quad v_n^2 = e^{j(\theta_n+\Delta\omega nT+\theta_0)} \quad (10)$$

where $p(\cdot)$ is the impulse response of a raised cosine pulse shaping system. Obviously, v_n^2 is not influenced by pulse shaping; and only v_n^1 value should be changed by removing ISI terms to get $v_n^{1'}$ defined as $e^{j(\theta_n+\Delta\omega(n-0.5)T+\theta_0)}$. Based on the fact that $p(0.5T)$ and $p(-0.5T)$ cause dominant ISI terms, v_n^1 is approximated as follows[1]:

$$v_n^1 \approx p(0.5T)e^{j(\theta_{n-1}+\Delta\omega(n-0.5)T+\theta_0)} + p(-0.5T)e^{j(\theta_n+\Delta\omega(n-0.5)T+\theta_0)} \quad (11)$$

[1]The expression in (11) is exact when the roll-off factor is 1.

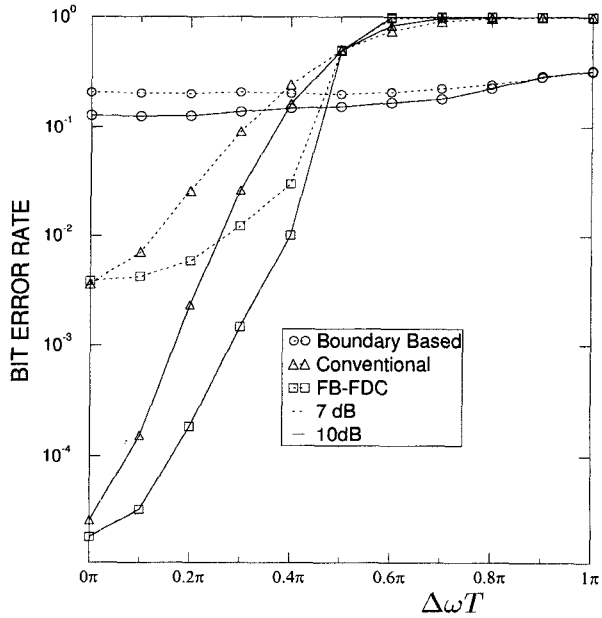

Fig.4. Empirical BER values of the boundary-based detector, the conventional detector and the one with FB-FDC, where dotted and solid lines show the BER values when SNR is 7dB and 10dB,respectively.

Since $p(0.5T) = p(-0.5T)$ and $e^{j(\theta_{n-1}+\Delta\omega(n-0.5)T+\theta_0)} \approx v_{n-1}^2$, we get

$$v_n^{1'} \approx \frac{v_n^1}{p(0.5T)} - v_{n-1}^2. \quad (12)$$

Following from (9) the boundary values for raised cosine pulses are given by

$$\hat{b}_n^i = v_n^{1'}; \quad \hat{b}_n^f = 2v_n^2 - v_n^{1'}. \quad (13)$$

C. Performance Evaluation of the Boundary-Based Detection

In order to evaluate the performance of the boundary-based detection, we generate *binary* DPSK symbols with 50 percent excess bandwidth raised cosine pulse shaping (roll-off factor=0.5). It was assumed that data were transmitted in short bursts of 64 bits. A total of 15000 bursts were generated and corrupted by additive white Gaussian noise (AWGN) and frequency shift. The corrupted bursts were passed through the boundary-based detector, and bit error rate (BER) values were estimated by counting the number of errors in demodulating the 15000 bursts. For comparison, the conventional DPSK receiver in Fig.1 and the one employing the FB-FDC in Fig.2 ($\alpha = 1/24$) were also considered. Fig.4 shows the results of this simulation. It is seen that the boundary-based detector performs

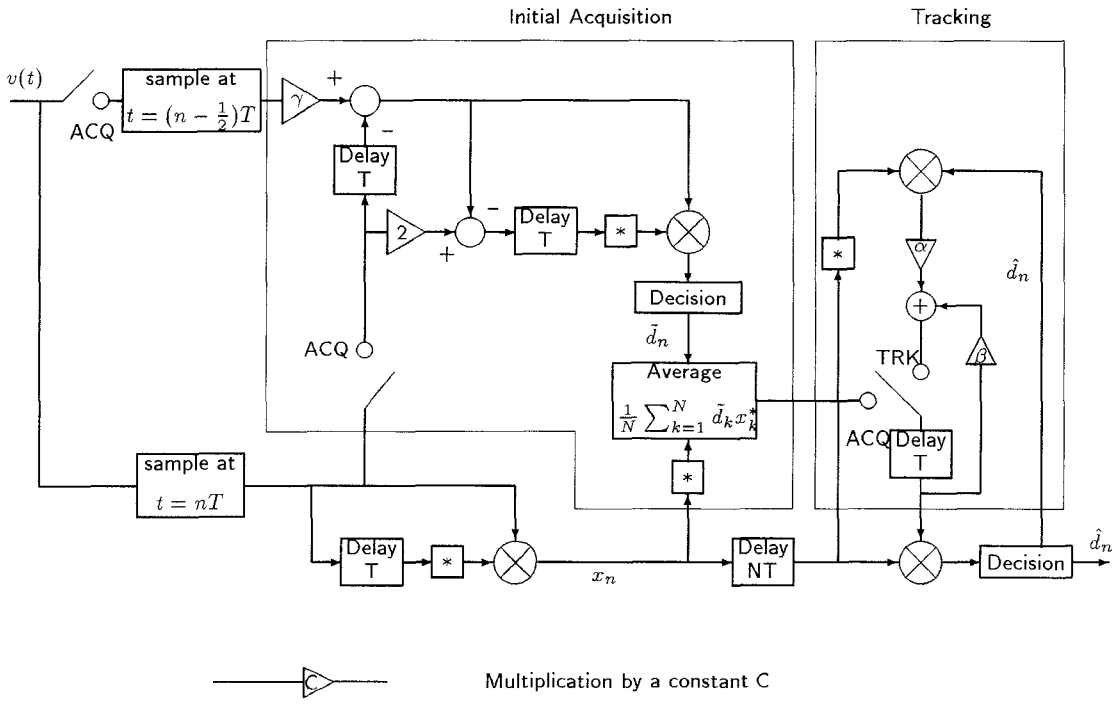

Fig.5. Entire Blockdiagram of the proposed DPSK Demodulator, where $\gamma = p(0.5T)^{-1}$. When the roll-off factor is 0.5, $\gamma = 1.667$.

considerably worse than the others when the frequency shift $\Delta\omega$ is small. This indicates that the former is vulnerable to AWGN. However, when $\Delta\omega T > 0.4\pi$ the boundary-based detector outperformed the others; in fact, its BER looks almost constant irrespective of $\Delta\omega T$. This result suggests that the boundary-based detector can be effective for initial acquisition of $\Delta\omega$.

IV. The Proposed DPSK Detector

A. The Algorithm

The demodulation scheme proposed in this section incorporates the boundary-based detection with the FB-FDC. Its entire blockdiagram is illustrated in Fig.5. At the beginning the switches in Fig.5 are connected to the ACQ positions and the initial value of $\hat{W}_n$ in (4), denoted by $\hat{W}_0$, is determined by using the boundary-based detector. Assuming a total of L DPSK symbols are transmitted, the procedure is stated as follows:

1) Sample $2N$ values at Nyquist rate over the first N symbol periods. Here $N << L$.

2) Apply the boundary-based detector to get an estimate of d_n defined in (2). This estimate is called the *tentative* estimate of d_n and denoted by $\tilde{d}_n$.

3) Since $d_n x_n^* = e^{j\Delta\omega T}$ from (2), we evaluate $\frac{1}{N}\sum_{k=1}^{N} \tilde{d}_n x_n^*$ and use this value as $\hat{W}_0$.

After obtaining $\hat{W}_0$ the two switches in Fig.5 providing data to the initial acquisition part are open and the one in the tracking part is connected to the TRK position. Then this system becomes the DPSK demodulator employing the FB-FDC with the initial value $\hat{W}_0$. This demodulation scheme is applied to the entire sequence sampled at $nT, n = 1, \cdots, L$. The "delay NT" block in Fig.5 is required to store the first N data which have been used for acquisition. Final output is the estimated sequence $\hat{d}_n, n = 1, \cdots, L$. Note that the tentative decision values $\tilde{d}_n, n = 1, \cdots, N$ obtained during acquisition are replaced with $\hat{d}_n$.

B. Performance Evaluation of the Proposed Detector

Inputs to the demodulator were generated as in Section III.C. Empirical BER values were evaluated for the proposed demodulator, the conventional one and the one employing the FB-FDC. We set $N = 32$ and $\alpha = 1/24$. The results shown in Fig.6 demonstrates that the proposed scheme can outperform the others for all $\Delta\omega T$ values and is indeed robust to frequency shift.

V. Conclusion

A new DPSK demodulation scheme which is robust to frequency shift was proposed and its performance was

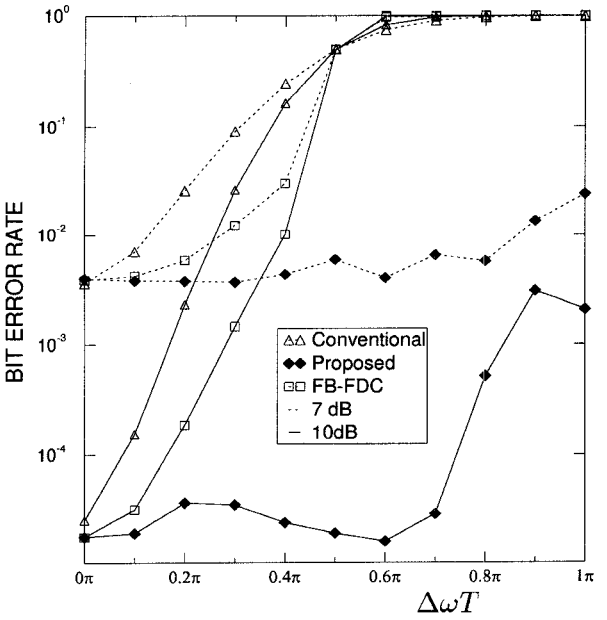

Fig.6. Empirical BER values of the conventional detector, the one with FB-FDC and the proposed detector, where dotted and solid lines show the BER values when SNR is 7dB and 10dB,respectively.

examined through computer simulation. This method performed better than existing techniques such as the one in [6] at the expense of higher sampling rate and some additional computation. It is expected that this method is particularly useful for applications that accompany excessive frequency shift.

References

[1] J. H.Park, Jr. "On Binary DPSK Detection," *IEEE Trans. Commun.*, vol. COM-26, No.4, pp. 484–486, April 1978.

[2] N. M. Blachman, "The effect of phase error on DPSK error probability," *IEEE Trans. Commun.*, vol. COM-29, pp. 364–365, Mar. 1981.

[3] R. F. Pawula, S. O. Rice, and J. H. Roberts, "Distribution of the phase angle between two vectors perturbed by gaussian noise," *IEEE Trans. Commun.*, vol. COM-30, pp. 1828–1841, Aug. 1982.

[4] F.D.Natali, "AFC Tracking Algorithms," *IEEE Trans. Commun.*, vol. COM-32, pp. 935–947, Aug. 1984.

[5] M. K. Simon, D. Divsalar, "Doppler-corrected differential detection of MPSK," *IEEE Trans. Commun.*, vol. 37, pp. 99–109, Feb. 1989.

[6] M. Ikura, et al., "Baseband processing frequency-drift-compensation for QDPSK signal transmission," *Electron. Lett.*, vol. 27, pp. 1521–1523, Aug. 1991.

[7] M. Ikura, et al., "Baseband-processing feedforward carrier frequency drift compensation for DPSK mobile radio," *Electron. Lett.*, vol. 28, pp. 771–773, Apr. 1992.

[8] M. Ikura and F. Adachi, "Baseband feedforward frequency drift compensation without false phase locking for burst DPSK signal reception," *Electron. Lett.*, vol. 28, pp. 1165–1167, Jun. 1992.

[9] S. Haykin, *Adaptive Filter Theory.* Englewood Cliffs, NJ: Prentice-Hall, 1991.

[10] P. J. Bickel and K. A. Doksum, *Mathematical Statistics: Basic ideas and selected topics.* San Francisco, CA: Holden-Day, Inc., 1977.